UDC 539.3 DOI: 10.32326/1814-9146-2022-84-3-409-419

COMPARATIVE ANALYSIS 1: INCIPIENT STAGE OF DYNAMIC DEFORMATION AND FRACTURE IN 1561 AND 1565 ALUMINUM ALLOYS

Meshcheryakov Yu.I.[1], Divakov A.K.[1], Zhigacheva N.I.[1], Konovalov G.V.[1], Osokin E.P.[2]

[1]*Institute for Problems of Mechanical Engineer in RAS, Saint-Petersburg, Russian Federation*
[2]*Central Research Institute of Constructional Materials “Prometei”, Saint-Petersburg, Russian Federation*

ym38@mail.ru

Received by the Editor 2022/06/15

Transition of dynamically deformed solids into structure-unstable state is analyzed theoretically and experimentally from the physical kinetics approach. Propagation of shock wave in heterogeneous medium is considered to be in the form of superposition of two modes: (i) propagation of plane front with the mean velocity $u(x,t)$ and (ii) random motions of local regions of medium because of chaotic stress fields. resulting from interaction of shock wave with the heterogeneous medium. This interaction results in particle velocity distribution, the quantitative characteristic of which is the particle velocity dispersion. Transition from one scale of dynamic deformation to another is found to be the so-called defect (decrease) of the particle velocity which characterizes the intensity of energy and momentum exchange between scale levels. Both characteristics are registered in real time in the process of shock-wave tests by using precise interferometric technique. Two materials, 1561 and 1565 aluminum alloys, were tested under uniaxial strain conditions within impact velocity range of 250–750 m/s. Owing to fine focusing of laser beam of interferometer up to 50–70 μm, the registered dynamic strength (spall strength) of material corresponds to single mesoscale structural element, which allows the incipient stage of dynamic fracture to be revealed in detail. The incipient strength is found to be maximum when velocity variation becomes equal to the velocity defect.

Keywords: multiscale deformation, velocity dispersion, velocity defect, aluminum alloys, spallation, insipient fracture.

Introduction

Development of the mechanics of deformed solid supposes incorporating the multiscale mechanisms of deformation and fracture both in quasistatics [1–3] and dynamics [4–7]. The multiscale mechanics implies a formation of intermediate scales between macroscale and microscale followed by transient non-equilibrium processes. At least three scale levels of quasistatic deformation have been recognized for over several decades: dislocation scale, mesoscale and macroscale. The shock-induced dynamic mesoparticles are shown to be nucleated in form of short (150–200 ns) single-sign dislocation pile-ups [8, 9]. The process of nucleation and propagation of pile-ups in heterogeneous medium results in particle velocity fluctuations which can be experimentally registered in the form of particle velocity distribution. The modern experimental techniques allow both the average particle velocity, u_{ms2}, and particle velocity variance, D_{ms1}, to be registered in real time [10–14]. Owing to focusing the laser beam of interferometer up to 50–70 μm the registered with the interferometer mean particle velocity concerns the motion of single structural element of mesoscale-2 whereas the velocity distribution at the mesoscale-1 corresponds to behavior of meso-1 particles inside of the mesoscale-2 element. The well-known criteria for dynamic fracture deal with the integral strength behavior of material - dynamic yield stress, dynamic toughness, spall strength and so on. The integral criteria do not incorporate the insipient stage of dynamic fracture. In the present study, as quantitative characteristic of intensity of momentum meso-macro exchange during the multiscale deformation and fracture, the *defect of particle velocity* is introduced. It is defined to be the difference between the velocity of impactor and maximum free surface velocity, $\Delta U = U_{\text{imp}} - U_{fs\,\text{max}}$.

The second dynamic characteristic which reflects a transition of material into structure-unstable state and characterizes the beginning of shock-induced structural heterogenization of material is the *threshold of structural instability* U_{ins}. The specifics of our experiments is that the laser beam spot of interferometer focused on to the free surface of target doesn't exceed 50–70 μm. The registered response of material on dynamic loading characterizes the tensile strength of single structural element, which corresponds to *incipient* stage of dynamic deformation and fracture.

1. Meso-macro momentum exchange and criterion for transition into structure-unstable state

Developed in the present study approach is based on three hypotheses followed from experimental and theoretical investigations of shock-wave processes in solids.

1. Propagation of shock wave in heterogeneous medium is considered to be in the form of superposition of two modes: (i) propagation of plane front with the mean velocity $u(x, t)$ and (ii) random motions of local regions of medium because of chaotic stress fields, which results in particle velocity distribution. The qualitative picture of multiscale shock front is presented in Fig. 1. In [15] this hypothesis has been used for description the meso-macro momentum exchange. The intensity of meso-macro momentum exchange was found to be characterized by the particle velocity defect ΔU:

$$\Delta U = \frac{1}{2}\frac{dD^2}{du}. \tag{1}$$

2. Particle velocity variation at the mesoscale (square root of the particle velocity dispersion), D, depends on the strain rate in the form [16]:

$$D = R\frac{d\varepsilon}{dt}. \tag{2}$$

An analogous dependence is known to exist in turbulence where the intensity of turbulent pulsations is proportional to acceleration of medium [17].

3. Mesoscale is subdivided by two sublevels: (i) mesoscale-1 (1–10) μm and (ii) mesoscale-2 (50–500) μm.

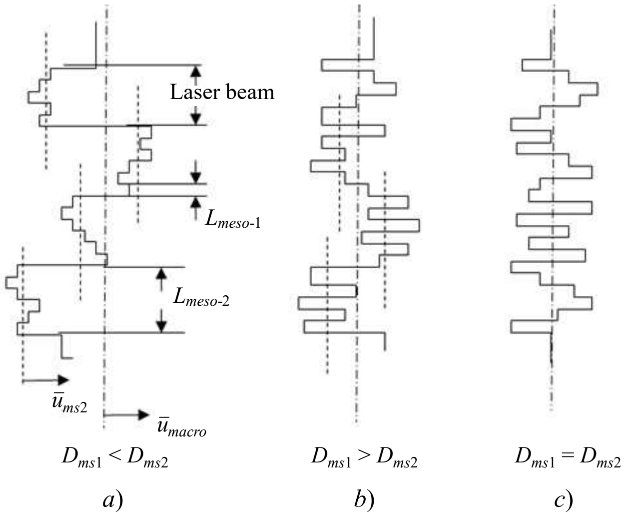

Fig. 1. Qualitative pattern of *U-L* velocity-space configurations of shock front for different relations between velocity dispersion the quantitative at mesoscale-1, D_{ms1}, and mesoscale-2, D_{ms2}

In the present study, as distinct from the well-known thermal approach [18, 19], the processes of dynamic deformation are considered from the position of physical kinetics [20]. In this approach, the random motions of particles are characterized by the particle velocity distribution function $f(r, v, t)$ and/or its statistical moments – mean particle velocity, $u(x, t)$, and particle velocity dispersion, $D^2(x, t)$:

$$u(x,t) = \int v f(x,v,t)\,dv; \tag{3}$$

$$D^2(x,t) = \int (v-u)^2 f(x,v,t) dv. \tag{4}$$

According to the physical kinetics approach, the scenario for developing the structural instability includes two stages:

1. Formation of the single-sign chaotically distributed dislocation pile-ups which are accepted to be the particles of mesoscale-1. The long-range interaction of pile-ups results in the mesoscale-1 velocity distribution (velocity dispersion).

2. At the critical strain rate, the velocity distribution transits into non-equilibrium stage. In this situation, the velocity defect, ΔU, emerges (Fig. 2).

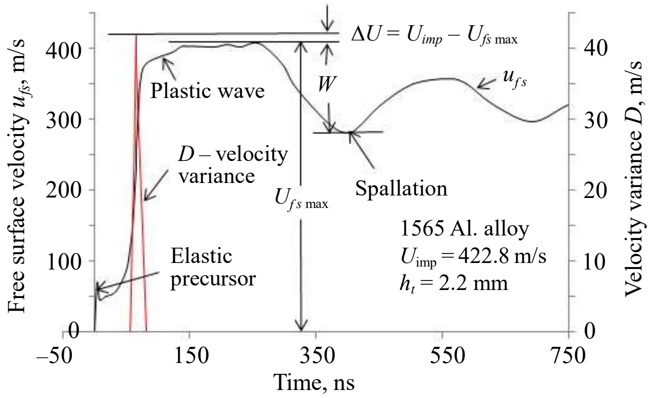

Fig. 2. The free surface velocity profile for the local point of target in 1565 aluminum alloy

Eq. (1) can be written in the form:

$$\Delta U = D\left(\frac{dD/dt}{du/dt}\right). \tag{5}$$

When the rate of change of velocity variance equals to the rate of change of mean particle velocity

$$\frac{dD}{dt} = \frac{du}{dt} \tag{6}$$

the velocity defect equals to the particle velocity variance:

$$\Delta U = D. \tag{7}$$

As the momentum exchange process requires a finite time Δt_f one can introduce an averaging of interscale momentum exchange over that time interval. The dynamic fracture is thought to happen when the following condition is fulfilled:

$$\int_{t-\tau}^{t}\left(\frac{1}{2}\frac{dD^2}{du}\right)dt' \le \Delta U_{cr}\tau, \tag{8}$$

where τ is the time interval for interscale momentum exchange and ΔU_{cr} is the critical value of the velocity defect. The multiplying of both sides of Eq. (8) by ρC_p, where ρ is a density of material, Cp is the velocity of shock wave, yields:

$$\rho C_p \int_{t-\tau}^{t}\left(\frac{1}{2}\frac{dD^2}{du}\right)dt' \le \Delta\sigma\tau, \tag{9}$$

where right hand side

$$\Delta\sigma\tau = \rho C_p \Delta U_{cr}\tau \tag{10}$$

is the momentum transferred from macroscale to mesoscale, whilst Eq. (8) can be considered as criterion for transition of solid into structure-unstable state.

2. Experimental results and analysis

Shock tests under uniaxial strain conditions were conducted with one-stage light gas gun of 37 mm barrel diameter. Two types of material, 1561 and 1565 aluminum alloys, were subjected to shock loading. The quasi-static mechanical characteristics of materials are provided in Table 1.

Table 1

Mechanical characteristics of aluminum alloys 1565 **and** 1561

Alloy	Target thickness, mm	σ_b, MPa	σ_{02}, MPa	δ, %
Al 1565	7	363	221	15.8
Al 1561	7	353–354	217–224	17.8–18.8

Data on dynamic strength and plasticity of material, including dynamic yield limit, spall strength, threshold of structural instability and particle velocity distribution are inferred from the temporal profiles of the mean free surface velocity, $u_{fs}(t)$, registered with the velocity interferometer In order to determine the instability threshold, a set of identical targets for both alloys were loaded within impact velocity range of 250–750 m/s. In Fig. 3, the dependencies of maximum free surface velocity, $U_{fs\,\max}$, for 1561 and 1565 aluminum alloys are plotted as functions of impact velocity. The dash line corresponds to the equality of impact velocity under symmetrical collision and maximum free surface velocity at the plateau of compression pulse ($U_{imp} = U_{fs\,\max}$). For 1565 aluminum alloy, the critical changes of slope for the maximum free surface velocity happen twice: at the impact velocity of 435 m/s (the free surface velocity equals 371.5 m/s) and velocity of 625.3 m/s (free surface velocity equals U_{ins} = 588.7 m/s. As for 1561 aluminum alloy, dependence $U_{fs\,\max} = f(U_{imp})$ does not contain the breaks. The maximum free surface velocity smoothly increases with the increasing of impact velocity.

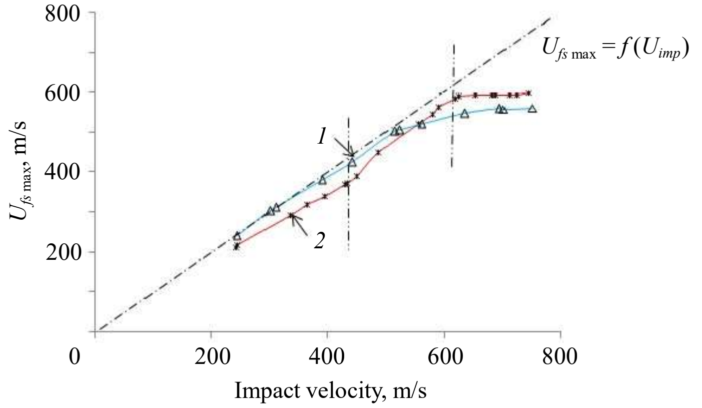

Fig. 3. Dependencies of maximum free surface velocity on impact velocity for 1561 (*1*) and 1565 (*2*) aluminum alloys

3. Structural instability and spall strength

While the threshold of structural instability characterizes the dynamic strength of material under compression, the spall strength is the tensile strength characteristic. In Fig. 4, the dependencies of the maximum free surface velocity at the plateau of compression pulse, $U_{fs\,\max}$, and pull-back velocity (spall strength), W, on the impact velocity for 1565 aluminum alloy are plotted together. The breaks on both curves happen at the identical impact velocities, which means that the internal processes responsible for dynamic deformation and strength for compression and tension for 1565 aluminum alloy are mutual related. When the material achieves the instability threshold, the spall strength decreases.

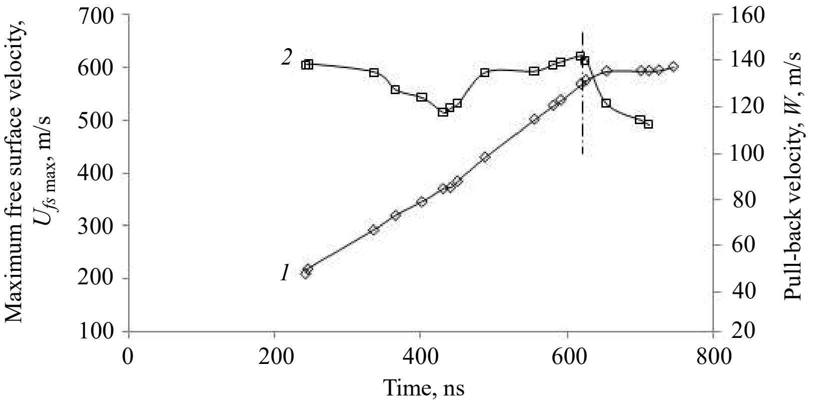

Fig. 4. Dependencies of maximum free surface velocity, $U_{fs\,\max}$ (*1*) and spall strength (pull-back velocity), W (*2*) on the impact velocity for 1565 aluminum alloy

For 1561 aluminum alloy, the dependence $W = f(U_{imp})$ could be built only up to impact velocity of 522.9 m/s (Fig. 5). In this material, at high impact velocities the laser beam of the interferometer reflected from the free surface of a target is deviated so the fringe signal disappears.

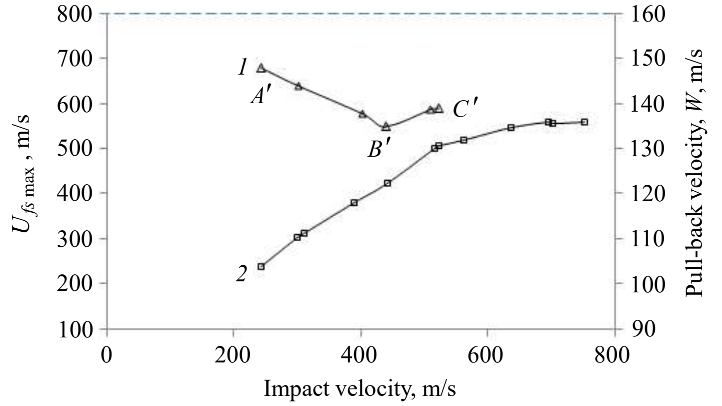

Fig. 5. Maximum free surface velocity, $U_{fs\ max}$, (*1*) and (pull-back velocity (spall strength), W, (*2*) versus impact velocity for 1561 aluminum alloy

The reason for loss of fringe signal in 1561 aluminum alloy target becomes clear after comparison of four characteristics: (i) spall strength $W=f(U_{imp})$, (ii) maximum free surface velocity, $U_{fs\ max}$, (iii) fringe signal and (iv) data on microstructural investigations of post shocked specimens Points C' in Fig. 5 indicates the maximum impact velocity at which the spall strength could be registered for 1561 alloy. This impact velocity corresponds to beginning of rotational motion of meso-2 structural element as a whole and to deviation of laser beam of interferometer. The rotational mechanism of medium is seen in post-shocked micrographs of 1561 aluminum alloy target. In our experiments, the post-shocked targets were cut along the impact direction and after polishing and etching in concentrated mixture of sulphuric and nitrogen asides were investigated with Axio-Observier Z-1m microscope.

In Fig. 6, the fringe signals for both type of alloys are provided. According to working principle of the interferometer, irreversible displacement of fringe signal to upper level of interference pattern means a loss of intensity of laser beam reflected from the free surface of the target.

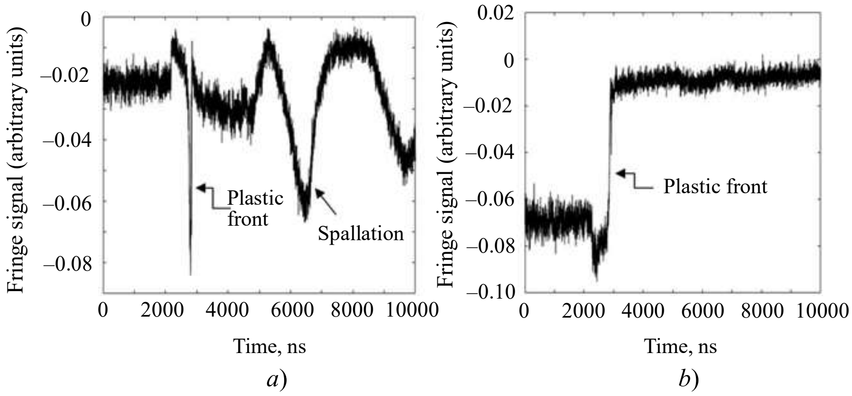

Fig. 6. Fringe signals for 1565 (*a*) and 1561 (*b*) aluminum alloys

In Fig. 7, the micrographs of initial state of grain structure for both alloys are presented. The inner structure of alloys is seen to differ very much – the grain structure of 1561 aluminum alloy consists of equal-axis grains whereas the structure of 1565 alloy contains the elongated grains (texture).

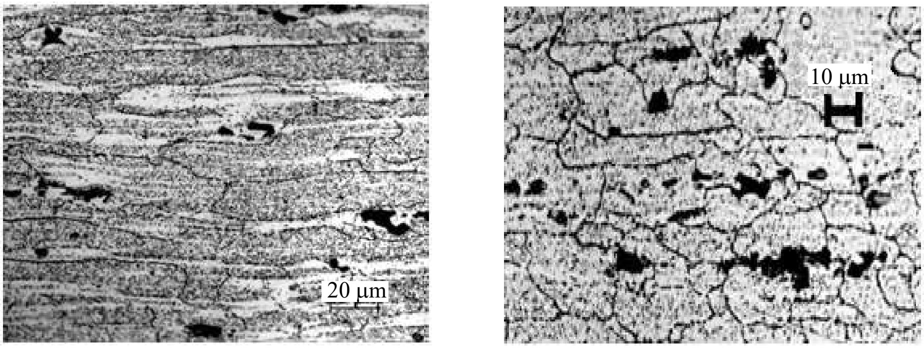

a) *b*)

Fig. 7. Initial state of structure for 1565 (*a*) and 1561 (*b*) aluminum alloys

As the interferometer registers of motion of single structural element of mesoscale-2, the rotation motion of the element in 1561 alloy (Fig. 8*a*) leads to deviation of laser beam and loss of the fringe signal. As for the 1565 alloy, dynamic deformation flows in form of translational motion of structural elements of mesoscale-2 (Fig. 8*b*). In this case, the deviation of laser beam at the free surface of target doesn't happen and free surface velocity profile can be registered within overall range of impact velocities. Such behavior of inner structure of 1565 alloy is related to texture of material which prevents to rotational motion of structural elements.

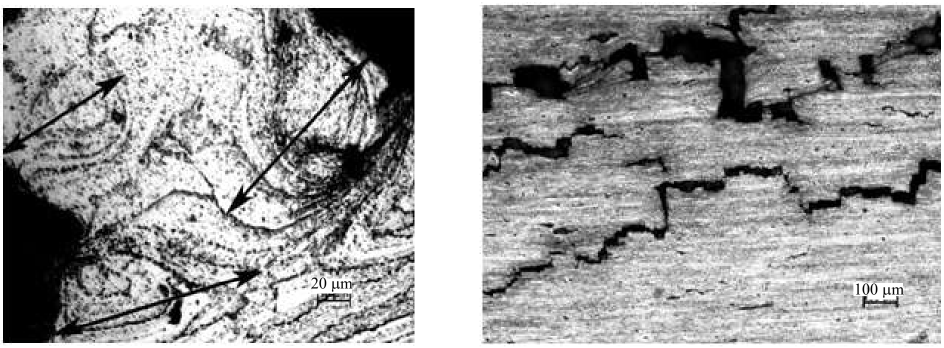

a) *b*)

Fig. 8. Morphology of spall zone in 1561 (*a*)
and 1565 (*b*) aluminum alloy targets (arrows indicate the rotation cells in 1561 alloy)

The meso-macro momentum exchange can explain a non-monotonous behavior of spall strength depending on the strain rate. The power balance at the spall zone can be written in the form:

$$\frac{1}{2}\rho C_p u^2 = \frac{1}{2}\mu\frac{u-\Delta U}{h}u + \frac{1}{2}\mu\frac{D}{h}u. \tag{11}$$

Here μ is a dynamic viscosity of deformed material, h is the width of spall zone and u is the mean particle velocity. The left hand side of Eq. (11) characterizes the power which is brought into spall zone from the shock wave. The right hand side of equation describes the lost of power due to normal rupture of material under tension at the spall zone and reflects a motion of spall surfaces in opposite directions. As particle velocity is currently changes owing to meso-macro momentum exchange, the strain rate includes the velocity defect, ΔU and the spherical component due to particle velocity distribution, so the total strain rate at the spall zone equals:

$$\frac{d\varepsilon}{dt} = \frac{u - (\Delta U - D)}{h}. \tag{12}$$

From (11) one obtains

$$h = \frac{\mu u (u - \Delta U + D)}{\rho C_p u}. \tag{13}$$

Time for spallation can be determined as

$$\tau = \frac{h}{u} = \frac{\mu}{\sigma}\left(1 - \frac{\Delta U - D}{u}\right),$$

$$\sigma\tau = \mu\left(1 - \frac{\Delta U - D}{u}\right), \tag{14}$$

where $\sigma = \rho C_p u$.

Dynamic generalization of this equation

$$\int_0^\tau \sigma dt' = \mu\left(1 - \frac{\Delta U - D}{u}\right) \tag{15}$$

can be considered as a *dynamic fracture criterion* which takes into account for the meso-macro momentum exchange. The dynamic strength is maximum when the particle velocity variance becomes equal to the velocity defect.

Conclusions

Transition of dynamically deformed solids into structure-unstable state is analyzed theoretically and experimentally from the physical kinetics approach. The kinetic criterion for transition of material into structure-unstable state includes the mesoparticle velocity distribution (mesoparticle velocity variation) and velocity defect (decrease) of stress pulse. Both characteristics can be registered in real time during the shock loading under uniaxial strain conditions. The local response of material on dynamic loading corresponds to incipient stage of multiscale dynamic deformation and fracture. The incipient strength is maximum when the mesoparticle velocity variation becomes equal to the particle velocity defect. The transition of material into structure-unstable state happens under the threshold strain rate at which the defect of particle velocity begins to grow abruptly. The local threshold of structural instability is found to be highly sensitive to initial morphology of material.

References

1. Panin V.E., Egorushkin V.E., Panin A.V. Fizicheskaya mezomekhanika deformiruemogo tverdogo tela kak mnogourovnevoy sistemy. 1. Fizicheskie osnovy mnogourovnevogo podkhoda [Physical mesomechanics of a deformed solid as a multilevel system. I. Physical fundamentals of

the multilevel approach]. *Fizicheskaya mezomekhanika* [*Physical Mesomechanics*]. 2006. Vol. 9. Iss. 3-4. P. 9–22 (In Russian).

2. Vladimirov V.I., Ivanov V.N., Priemskii N.M. Mezoskopicheskiy uroven deformatsii [Mesoscopic level of plastic deformation]. In: *Fizika prochnosti i plastichnosti* [*Physics of Strength and Plasticity*]. Ed. S.I. Zhurkov. Leningrad. Nauka Publ. 1986. P. 69–80 (In Russian).

3. Makarov P.V. Physical mesomechanic approach in simulation of deformation and fracture processes. *Phys. Mesomech*. 1998. Vol. 1. No 1. P. 57–75.

4. Chhabildas L.C., Trott W.M., Reinhart W.D., Cogar I.R., Mann G.A. Incipient spall structures in tantalum- microstructural effects. *Shock Compression of Condenced Matter-2001*. Eds. M.D. Funish, N.N. Thadani, Y.-Y. Horie. 24–29 June 2001. Atlanta. 2001. P. 483–486.

5. Baer M.R. Computatinal modeling of heterogeneous reactive materials at the mesoscale. *Shock Compression of Condenced Matter-1999: The APS Proceedings.* Eds. M.D. Furnish, L.C. Chhabildas, R.S. Nixon. New York. 1999. P. 27–33.

6. Vogler T.J., Reinhart W.D., Chhabildas L.C. Dynamic behavior of boron carbide. *J. Appl. Phys*. 2004. Vol. 95. Iss. 8. P. 4173–4183. DOI: 10.1063/1.1686902.

7. Yano K., Horie Y. Discrete-element modeling of shock compression of polycrystalline copper. *Phys. Rev. B.* 1999. Vol. 59. Iss. 21. P. 13672–13680. https://doi.org/10.1103/PhysRevB.59.13672.

8. Meshcheryakov Yu.I., Prokuratova E.I. Kinetic theory of continuously distributed dislocations. *Int. J. Solids Struct*. 1995. Vol. 32. No 12. P. 1711–1726.

9. Prokuratova E.I., Indeitzev D.A. The conditions for the dislocation distribution localization under dynamic loading. *Dymat Journal.* 1995. Vol. 2. No 3/4. P. 229–233.

10. Barker L.M. Fine structure of compressive and release wave shape in aluminum measured by the velocity interferometer technique. *Symposium on High Dynamic Pressure*. Paris. 1967. P. 369–382. DOI: 10.2172/4322636.

11. Zlatin N. A., Pugachev G.S., Volovetz L.D., Zilberbrand E.L., Leontiev S.A. Interferometricheskaya registratsiya parametrov slabykh voln napryazheniy v tverdykh telakh [Interferometric registration of parameters of weak stress waves in solids]. *Zhurnal tekhnicheskoy fiziki* [*Soviet Physics. Technical Physics*]. 1981. Vol. 51. No 7. P. 1503–1506 (In Russian).

12. Zlatin N.A., Mochalov C.M., Pugachev G.S., Bragov A.M. Laser differential interferometer. *Soviet Physics. Technical Physics*. 1974. Vol. 18. No 9. P. 1235–1237.

13. Asay J.R., Barker L.M. Interferometric measurements of shock-induced internal particle velocity and spatial variation of particle velocity. *J. Appl. Phys.* 1974. Vol. 45. Iss. 6. P. 2540–2546. DOI: 10.1063/1.1663627.

14. Meshcheryakov Yu.I., Divakov A.K. Multi-scale kinetics of microstructure and strain-rate dependence of materials. *Dymat Journal*. 1994. Vol. 1. (4). P. 271–287.

15. Meshcheryakov Yu.I., Divakov A.K., Zhigacheva N.I., Makarevich I.P., Barakhtin B.K. Dynamic structures in shock-loaded copper. *Phys. Rev. B.* 2008. Vol. 78. P. 64301–64316. DOI: 10.1103/PHYSREVB.78.064301.

16. Indeitzev D.A., Meshcheryakov Yu.I., Kuchmin A.Yu., Vavilov D.S. Multi-scale model of steady-wave shock in a medium with relaxation. *Acta Mech.* 2015. Vol. 226. Iss. 3. P. 917–925. DOI: 10.1007/S00707-014-1231-0.

17. Hintze J.O. *Turbulence.* New York. Graw Hill Inc. 1962. 680 p.

18. Grady D.E., Asay J.R. Calculation of thermal trapping in shock deformation of aluminum. *J. Appl. Phys.* 1982. Vol. 53. Iss. 1. P. 7350–7354. DOI: 10.1063/1.330101.

19. Grady D.E., Kipp M.E. The growth of unstable thermoplastic shear with application to steady-wave shock compression in solids. *J. Mech. Phys. Solids*. 1987. Vol. 35. Iss 1. P. 95–119. http://doi.org/10.1016/0022-5096(87)90030-5.

20. Meshcheryakov Yu.I. Kinetic theory of dislocations and mesoscale formation in dynamically deformed solids. In: *Advanced Structured Materials*. Vol. 103. Springer Nature. 2019. P. 395–412. http://doi.org/10.1007/978-3-030-11665-1_22.

Список литературы

1. Панин В.Е., Егорушкин В.Е., Панин А.В. Физическая мезомеханика деформируемого твердого тела как многоуровневой системы. 1. Физические основы многоуровневого подхода. *Физическая мезомеханика.* 2006. Т. 9. №3-4. С. 9–22.

2. Владимиров В.И., Иванов В.Н., Приемский Н.М. Мезоскопический уровень деформации. В кн.: *Физика прочности и пластичности*. Под ред. С.И. Журкова. Л.: Наука, 1986. С. 69–80.

3. Makarov P.V. Physical mesomechanic approach in simulation of deformation and fracture processes. *Physical Mesomechanics*. 1998. Vol. 1. No 1. P. 57–75.

4. Chhabildas L.C., Trott W.M., Reinhart W.D., Cogar I.R., Mann G.A. Incipient spall structures in tantalum- microstructural effects. *Shock Compression of Condenced Matter-2001*. Eds. M.D. Funish, N.N. Thadani, Y.-Y. Horie. 24–29 June 2001. Atlanta, 2001. P. 483–486.

5. Baer M.R. Computatinal modeling of heterogeneous reactive materials at the mesoscale. *Shock Compression of Condenced Matter-1999: The APS Proceedings*. Eds. M.D. Furnish, L.C. Chhabildas, R.S. Nixon. New York, 1999. P. 27–33.

6. Vogler T.J., Reinhart W.D., Chhabildas L.C. Dynamic behavior of boron carbide. *Journal of Applied Physics*. 2004. Vol. 95. Iss. 8. P. 4173–4183. DOI: 10.1063/1.1686902.

7. Yano K., Horie Y. Discrete-element modeling of shock compression of polycrystalline copper. *Physical Review B*. 1999. Vol. 59. Iss. 21. P. 13672–13680. https://doi.org/10.1103/PhysRevB.59.13672.

8. Meshcheryakov Yu.I., Prokuratova E.I. Kinetic theory of continuously distributed dislocations. *International Journal of Solids and Structures*. 1995. Vol. 32. No 12. P. 1711–1726.

9. Prokuratova E.I., Indeitzev D.A. The conditions for the dislocation distribution localization under dynamic loading. *Dymat Journal*. 1995. Vol. 2. No 3/4. P. 229–233.

10. Barker L.M. Fine structure of compressive and release wave shape in aluminum measured by the velocity interferometer technique. *Symposium on High Dynamic Pressure*. Paris. 1967. P. 369–382. DOI: 10.2172/4322636.

11. Златин Н.А., Пугачев Г.С., Воловец Л.Д., Зильбербрант Е.Л., Леонтьев С.А. Интерферометрическая регистрация параметров слабых волн напряжений в твердых телах. *ЖТФ*. 1981. Т. 51. №7. С. 1503–1506.

12. Златин Н.А., Мочалов С.М., Пугачев Г.С., Брагов А.М. Лазерный дифференциальный интерферометр. *ЖТФ*. 1973. Т. 49. Вып. 9. С. 194–205.

13. Asay J.R., Barker L.M. Interferometric measurements of shock-induced internal particle velocity and spatial variation of particle velocity. *Journal of Applied Physics.* 1974. Vol. 45. Iss. 6. P. 2540–2546. DOI: 10.1063/1.1663627.

14. Meshcheryakov Yu.I., Divakov A.K. Multi-scale kinetics of microstructure and strain-rate dependence of materials. *Dymat Journal.* 1994. Vol. 1. (4). P. 271–287.

15. Meshcheryakov Yu.I., Divakov A.K., Zhigacheva N.I., Makarevich I.P., Barakhtin B.K. Dynamic structures in shock-loaded copper. *Physical Review. B*. 2008. Vol. 78. P. 64301–64316. DOI: 10.1103/PHYSREVB.78.064301.

16. Indeitzev D.A., Meshcheryakov Yu.I., Kuchmin A.Yu., Vavilov D.S. Multi-scale model of steady-wave shock in a medium with relaxation. *Acta Mechanica*. 2015. Vol. 226. Iss. 3. P. 917–925. DOI: 10.1007/S00707-014-1231-0.

17. Hintze J.O. *Turbulence.* New York: Graw Hill Inc., 1962. 680 p.

18. Grady D.E., Asay J.R. Calculation of thermal trapping in shock deformation of aluminum. *Journal of Applied Physics*. 1982. Vol. 53. Iss. 1. P. 7350–7354. DOI: 10.1063/1.330101.

19. Grady D.E., Kipp M.E. The growth of unstable thermoplastic shear with application to steady-wave shock compression in solids. *Journal of the Mechanics and Physics of Solids*. 1987. Vol. 35. Iss 1. P. 95–119. http://doi.org/10.1016/0022-5096(87)90030-5.

20. Meshcheryakov Yu.I. Kinetic theory of dislocations and mesoscale formation in dynamically deformed solids. In: *Advanced Structured Materials*. Vol. 103. Springer Nature, 2019. P. 395–412. http://doi.org/10.1007/978-3-030-11665-1_22.

СРАВНИТЕЛЬНЫЙ АНАЛИЗ 1: НАЧАЛЬНАЯ СТАДИЯ ДИНАМИЧЕСКОГО ДЕФОРМИРОВАНИЯ И РАЗРУШЕНИЯ АЛЮМИНИЕВЫХ СПЛАВОВ 1561 И 1565

Мещеряков Ю.И.[1], Диваков А.К.[1], Жигачева Н.И.[1], Коновалов Г.В.[1], Осокин Е.П.[2]

[1]*Институт проблем машиноведения РАН, Санкт-Петербург, Российская Федерация*
[2]*ЦНИИ конструкционных материалов «Прометей», Санкт-Петербург, Российская Федерация*

С позиции физической кинетики анализируется переход динамически деформируемых твердых тел в структурно-неустойчивое состояние. Распространение ударной волны в структурно-неоднородной среде рассматривается в виде суперпозиции двух мод движения: распространение плоского волнового фронта со средней скоростью $u(x, t)$ и случайные движения локальных областей деформируемой среды как результат взаимодействия ударной волны со структурно-неоднородной средой. Последний тип взаимодействия приводит к распределению частиц среды по скоростям, которое количественно характеризуется в виде дисперсии массовой скорости. Переход с одного масштабного уровня динамического деформирования на другой сопровождается появлением так называемого дефекта массовой скорости, который определяет интенсивность обмена энергией и количеством движения между масштабными уровнями. Обе динамические характеристики регистрируются в реальном масштабе времени с помощью лазерного дифференциального интерферометра. Два типа материала, алюминиевые сплавы 1561 и 1565, испытаны в условиях одноосной деформации (плоского соударения) в диапазоне скоростей ударника 250–750 м/с. Благодаря тонкой фокусировке лазерного луча на тыльной поверхности мишени (50–70 мкм), регистрируемый интерферометром отклик материала на ударное нагружение соответствует ударно-волновому поведению одного структурного элемента мезоуровня, что отвечает начальной стадии динамического деформирования и разрушения материала. Экспериментально показано, что динамическая прочность такого структурного элемента максимальна в том случае, когда вариация массовой скорости на мезоуровне равна дефекту массовой скорости на плато импульса сжатия.

Ключевые слова: многомасштабная деформация, дисперсия скорости, дефект скорости, алюминиевые сплавы, откольное разрушение, начальная стадия разрушения.